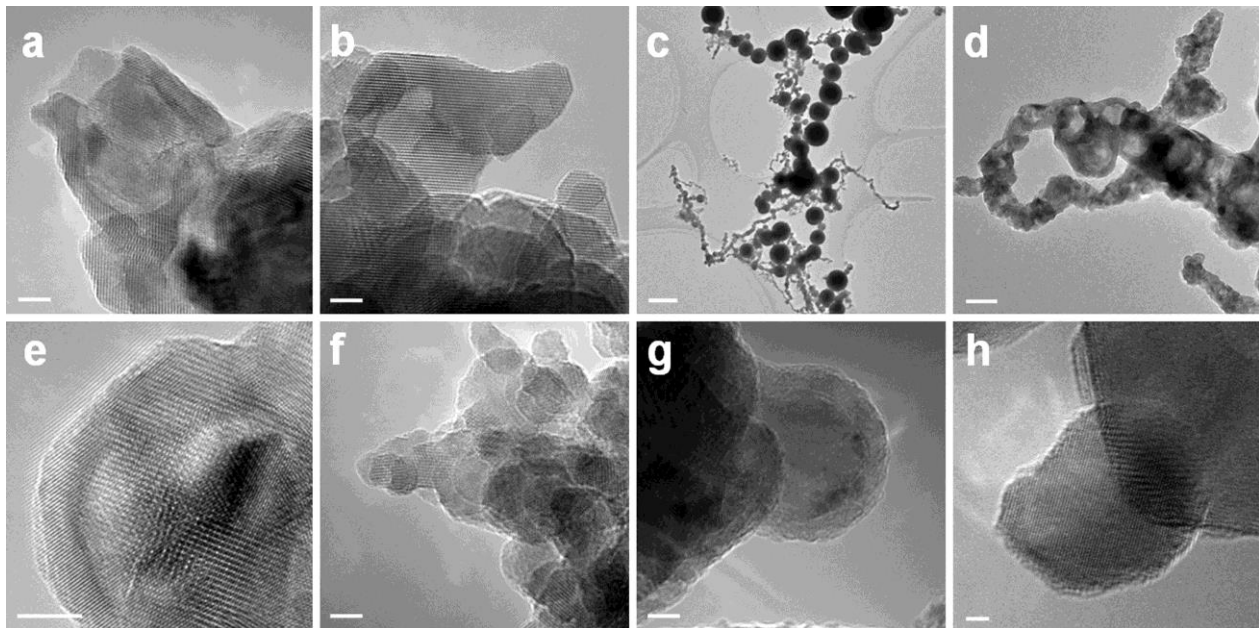
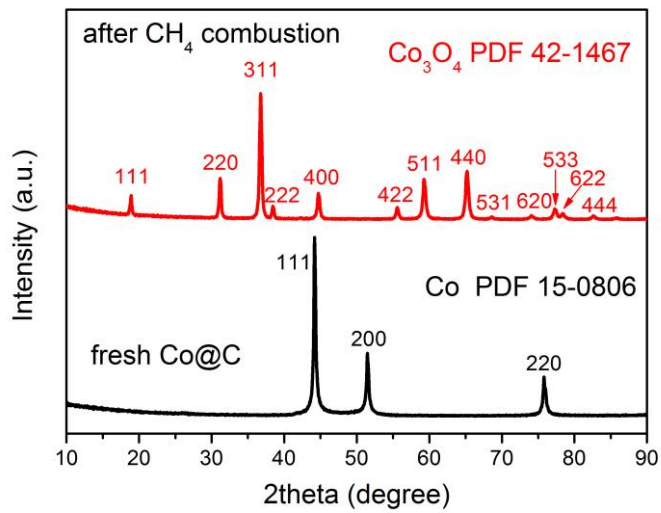


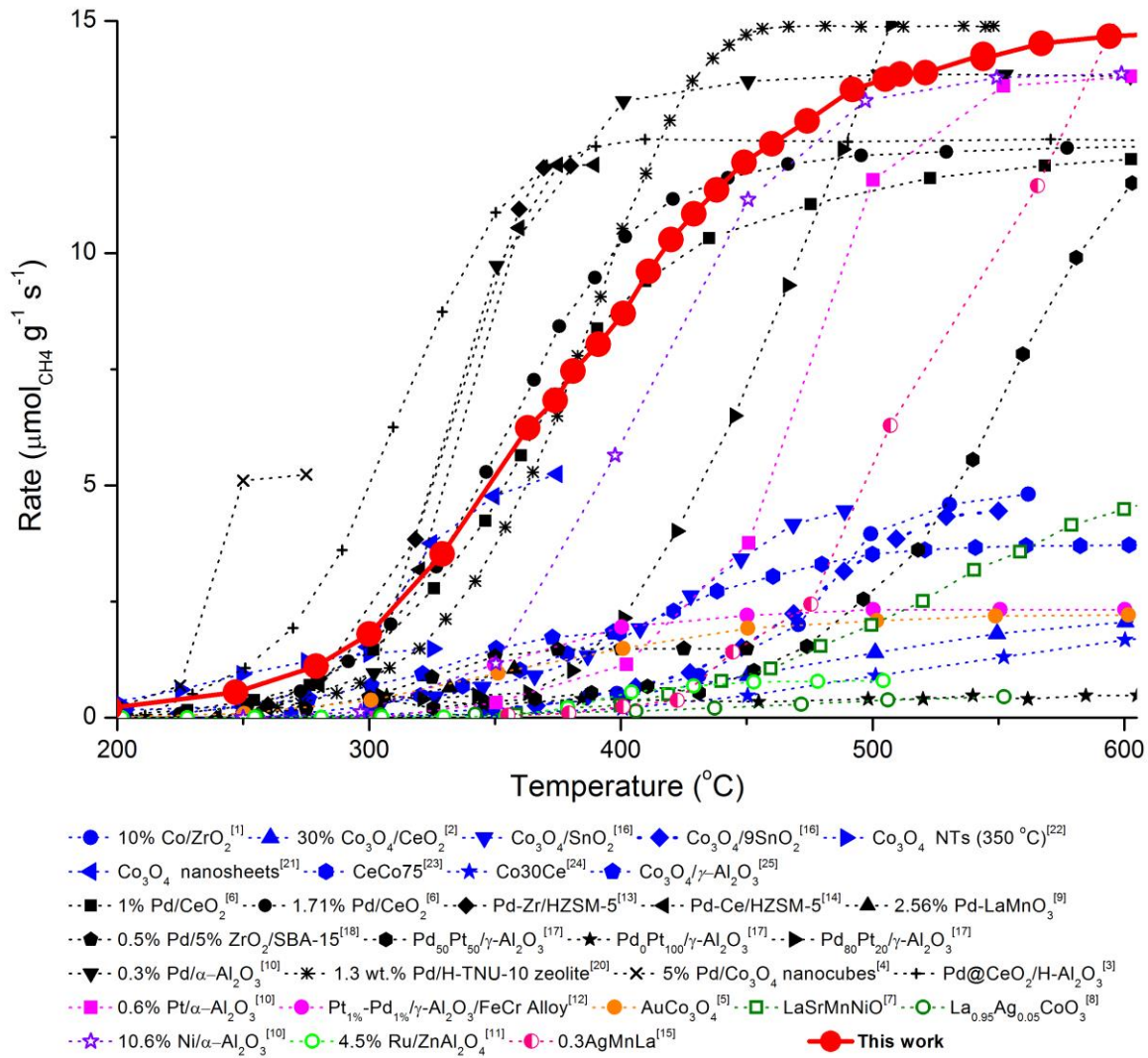
## Supplementary Information:



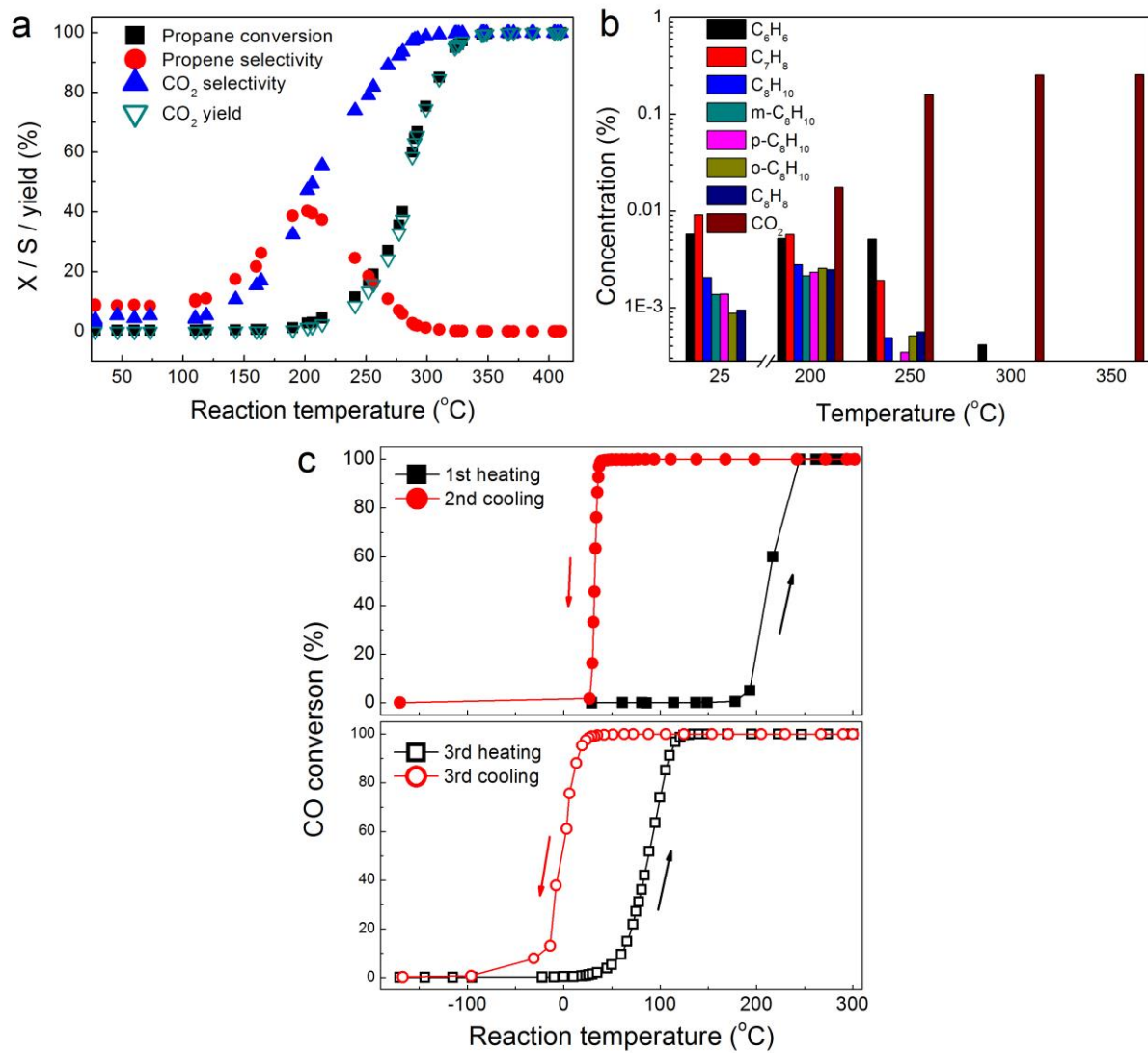
**Supplementary Figure 1. TEM images.** Co@C nanocapsules oxidized at (a, e) 300 °C and (b, f) 400 °C. Carbon-free Co nanoparticles oxidized at (c, g) 20 °C and (d, h) 450 °C. The carbon-free Co nanoparticles were synthesized by the same process without using ethanol. Scale bars, 5 nm (in a, b, e-g), 500 nm (in c), 50 nm (in d) and 2 nm (in h).



**Supplementary Figure 2. Powder XRD patterns of the fresh and reacted Co@C samples.** The curves of fresh and reacted samples were matched well with that of metallic cobalt (PDF 15-0806) and cobalt oxide (PDF 42-1467), respectively.



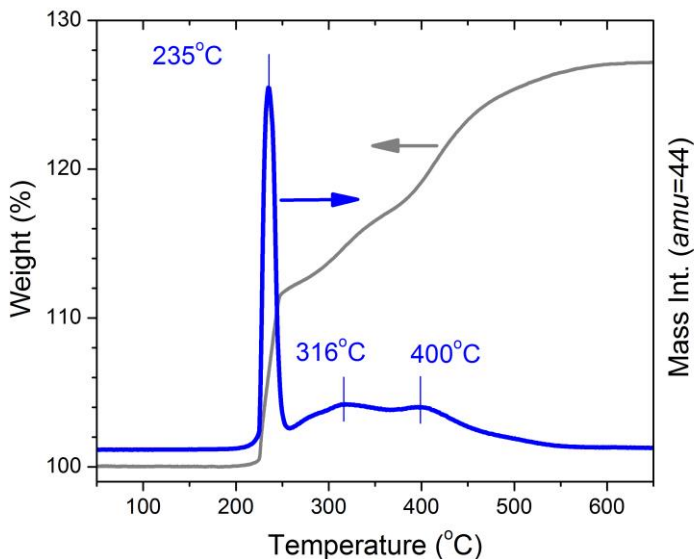
**Supplementary Figure 3. Catalytic performance comparison with references<sup>1-25</sup>.** The CH<sub>4</sub> reaction rates were calculated based on the total mass of these catalysts.



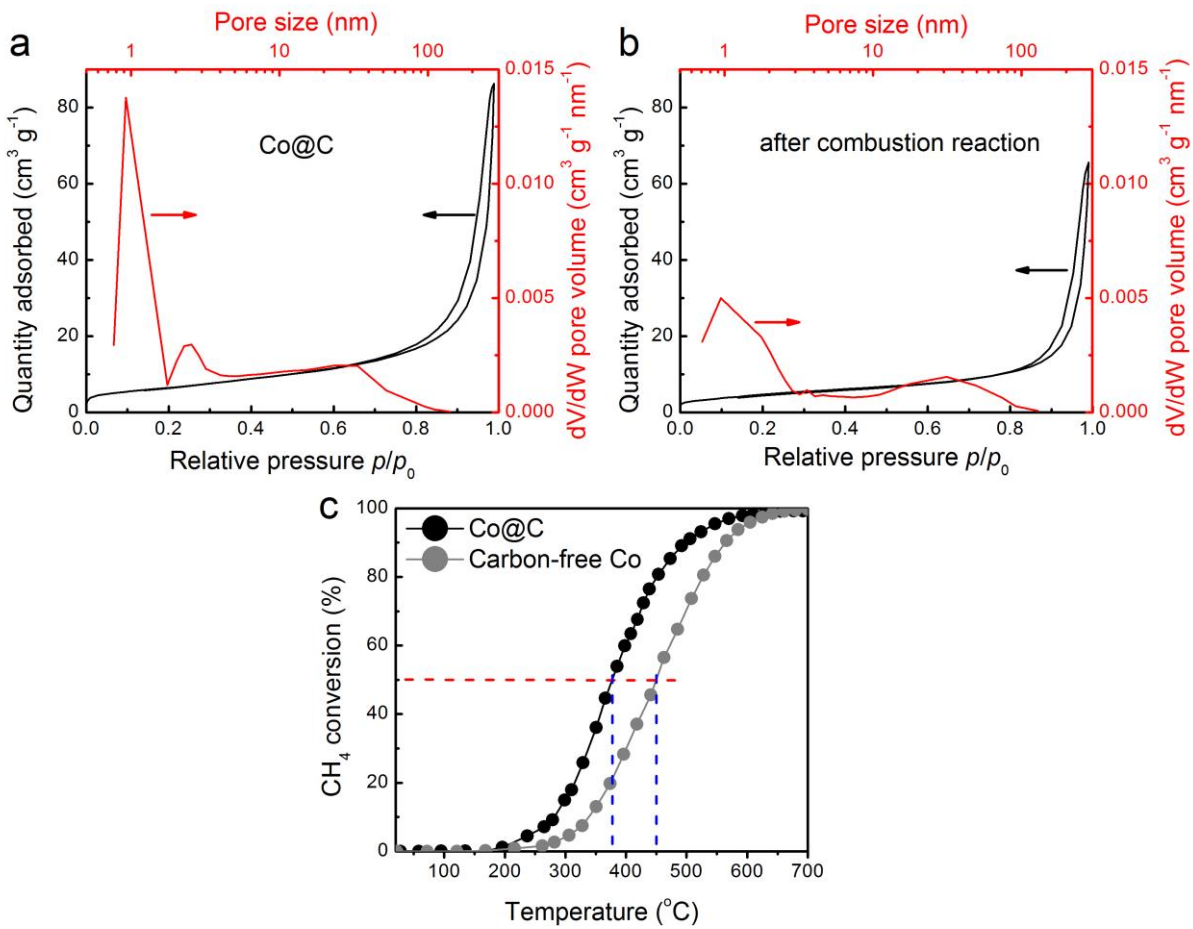
**Supplementary Figure 4. Catalytic performances in combustion of propane, aromatics and carbon monoxide.**

(a) Propane conversion ( $X$ ), propene selectivity ( $S$ ), CO<sub>2</sub> selectivity ( $S$ ) and yield as a function of reaction temperature obtained from room temperature to 420 °C over 100 mg Co@C catalyst, 2.6% C<sub>3</sub>H<sub>8</sub> with excess oxygen.

(b) Concentration of aromatic mixture and yielded CO<sub>2</sub> against the reaction temperature over 100 mg Co@C catalyst with excess oxygen. (c) Heating and cooling light-off curves of CO oxidation against the reaction temperature over 100 mg Co@C with 1.24% CO and 3.10% O<sub>2</sub> in helium at the total GHSV of 12.2 L g<sup>-1</sup> h<sup>-1</sup>. We note that the residual carbon shells may block the diffusion of reactant onto the active sites, resulting in an underestimation of the catalytic activity.



**Supplementary Figure 5. Temperature-programmed oxidation of pristine Co@C sample in a flow of diluted oxygen.** The pristine nanocapsules showed the chemical and thermal stability at the low temperature below 200 °C. When the temperature elevated from 220 °C to 600 °C, a total weight gain of about 27 wt% on the TG curve arises with synchronous changes in escaping CO<sub>2</sub> MS signals.



**Supplementary Figure 6. Textural structure and catalytic performance of Co@C and carbon-free Co nanoparticles.** N<sub>2</sub> physisorption results of Co@C samples (a) before and (b) after reaction. (c) Light-off curves of Co@C and carbon-free Co. We noted that the BET surface area and pore volume were 23.3  $\text{m}^2 \text{g}^{-1}$ , 0.134  $\text{mL g}^{-1}$  for the pristine Co@C and 17.5  $\text{m}^2 \text{g}^{-1}$ , 0.102  $\text{mL g}^{-1}$  for the used sample, respectively. The  $T_{50}$  values of catalytic combustion reaction were 376 °C and 450 °C, while the CH<sub>4</sub> conversion were 50% and 20.2% at 376 °C on Co@C and carbon-free Co catalysts, respectively.

**Supplementary Table 1. Comparison of TOF and kinetic parameters with references.**

Catalyst	TOF (s <sup>-1</sup> )	CH <sub>4</sub> reaction order	O <sub>2</sub> reaction order	Activation energy kJ mol <sup>-1</sup>	Reference
Co <sub>3</sub> O <sub>4</sub>	0.016 <sup>a</sup> (533K)	0.652	0.003	68±1	This work
Co(1.9)/ZrO <sub>2</sub>	—	—	—	108.68	26
Co(0.9)La/ZrO <sub>2</sub>	—	—	—	121.22	
Co-Mg/Al ternary hydrotalcites	—	—	—	86~134	27
aCoO <sub>3</sub> (a=La, Pr, Nd, and Gd)	—	—	—	98.6~110	28
ZrLaMn <sub>x</sub> (x=2,4,6,12,16)	—	0.79~0.82	—	85.2~100.9	29
LaMnO <sub>3</sub>	—	0.83	—	97.5	
Pt/ $\gamma$ -Al <sub>2</sub> O <sub>3</sub>	0.0015	—	—	67~138	30
Pd wire	5.4 (673K)	0.8	0.1	71.0	31
Pt wire	0.13 (773K)	1.0	-0.6	87.8	
Rh wire	0.52 (773K)	0.6	0	100	
0.038~1.0wt% Pd/Al <sub>2</sub> O <sub>3</sub>	0.024~0.31 (673K)	0.6~0.8	0~0.1	71~84	
0.22wt% Pt/Al <sub>2</sub> O <sub>3</sub>	0.048~0.14 (773K)	1.1~1.2	-0.6 ~ -0.5	100	
0.03~1.153wt% Rh/Al <sub>2</sub> O <sub>3</sub>	0.048~0.14 (773K)	0.4~0.5	0~0.1	92~96	
Pd(111)	2.8-2.9 (598K)	0.8	-0.1	140 ± 20	32
Pd(100)	5.0-5.3 (598K)	0.8	0.1	125 ± 15	
Pd(110)	1.2-1.4 (598K)	0.7	0.2	160 ± 20	
2.7wt% Pd/ $\gamma$ -Al <sub>2</sub> O <sub>3</sub>	2.28 (623K)	1.0	0	84 ± 3 (<680 K); 23 ± 2 (>680 K)	33
3.3wt% Pd/ $\gamma$ -Al <sub>2</sub> O <sub>3</sub>	0.03-0.29 (473K)	0.95	0.86	78.6 ± 5.0	34
1.0~10.0wt% Pd/ $\gamma$ -Al <sub>2</sub> O <sub>3</sub>	—	1.0	0	76 (473-673K)	35
Pd/H-TNU-10	0.171 (673K)	0.6	0.0	78	20
Pd/H-ZSM-5(II)	0.109 (673K)	0.5	-0.2	84	
Pd/H-mordenite	0.075 (673K)	0.7	-0.1	77	
Pd/H-beta	0.068 (673K)	0.5	0.2	72	
Pd(1%)@CeO <sub>2</sub> (9%)/H-Al <sub>2</sub> O <sub>3</sub>	0.047	—	—	103 (493~543K)	3
Pd(1%)/CeO <sub>2</sub> IWI	0.0013	—	—	90(493~543K)	
Pd(1%)/CeO <sub>2</sub> (9%)/Al <sub>2</sub> O <sub>3</sub> IMP	0.0015	—	—	120(523~563K)	
0.5~4.5wt% Ru/ZnAl <sub>2</sub> O <sub>4</sub>	0.006~0.010 (648K)	—	—	124~129	11

<sup>a</sup>The surface area of cobalt was measured by the CO chemisorption test according to Ref. 36. The density of active sites is 51.9 μmol<sub>Co</sub> g<sup>-1</sup>.

## Supplementary References

1. Xiao, T. C., Ji, S. F., Wang, H. T., Coleman, K. S. & Green, M. L. H. Methane combustion over supported cobalt catalysts. *J. Mol. Catal. A* **175**, 111-123 (2001)
2. Liotta, L. F., Di Carlo, G., Pantaleo, G. & Deganello, G. Catalytic performance of  $\text{Co}_3\text{O}_4/\text{CeO}_2$  and  $\text{Co}_3\text{O}_4/\text{CeO}_2\text{-ZrO}_2$  composite oxides for methane combustion: Influence of catalyst pretreatment temperature and oxygen concentration in the reaction mixture. *Appl. Catal. B* **70**, 314-322 (2007)
3. Cargnello, M. *et al.* Exceptional activity for methane combustion over modular  $\text{Pd}@\text{CeO}_2$  subunits on functionalized  $\text{Al}_2\text{O}_3$ . *Science* **337**, 713-717 (2012)
4. Hu, L. H., Peng, Q. & Li, Y. D. Low-temperature  $\text{CH}_4$  catalytic combustion over Pd catalyst supported on  $\text{Co}_3\text{O}_4$  nanocrystals with well-defined crystal planes. *Chemcatchem* **3**, 868-874 (2011)
5. Liotta, L. F., Di Carlo, G., Longo, A., Pantaleo, G. & Venezia, A. M. Support effect on the catalytic performance of  $\text{Au}/\text{Co}_3\text{O}_4\text{-CeO}_2$  catalysts for CO and  $\text{CH}_4$  oxidation. *Catal. Today* **139**, 174-179 (2008)
6. Colussi, S. *et al.* Nanofaceted Pd-O Sites in Pd-Ce surface superstructures: Enhanced activity in catalytic combustion of methane. *Angew. Chem. Int. Ed.* **48**, 8481-8484 (2009)
7. Alifanti, M., Kirchnerova, J., Delmon, B. & Klvana, D. Methane and propane combustion over lanthanum transition-metal perovskites: Role of oxygen mobility. *Appl. Catal. A* **262**, 167-176 (2004)
8. Buchneva, O. *et al.* La-Ag-Co perovskites for the catalytic flameless combustion of methane. *Appl. Catal. A* **370**, 24-33 (2009)
9. Cimino, S., Casaleotto, M. P., Lisi, L. & Russo, G. Pd-LaMnO<sub>3</sub> as dual site catalysts for methane combustion. *Appl. Catal. A* **327**, 238-246 (2007)
10. Li, B. T. *et al.* High combustion activity of methane induced by reforming gas over Ni/Al<sub>2</sub>O<sub>3</sub> catalysts. *Appl. Catal. A* **290**, 36-45 (2005)
11. Okal, J. & Zawadzki, M. Catalytic combustion of methane over ruthenium supported on zinc aluminate spinel. *Appl. Catal. A* **453**, 349-357 (2013)
12. Maione, A., Andre, F. & Ruiz, P. Structured bimetallic Pd-Pt/ $\gamma$ -Al<sub>2</sub>O<sub>3</sub> catalysts on FeCrAlloy fibers for total combustion of methane. *Appl. Catal. B* **75**, 59-70 (2007)
13. Shi, C. K., Yang, L. F., He, X. E. & Cai, J. X. Enhanced activity and stability of Zr-promoted Pd/HZSM-5 catalyst for low-temperature methane combustion. *Chem. Commun.* 2006-2007 (2002)
14. Shi, C. K., Yang, L. F. & Cai, J. X. Cerium promoted Pd/HZSM-5 catalyst for methane combustion. *Fuel* **86**, 106-112 (2007)
15. Machocki, A. *et al.* Manganese-lanthanum oxides modified with silver for the catalytic combustion of methane. *J. Catal.* **227**, 282-296 (2004)
16. Tang, X. F., Hao, J. M. & Li, J. H. Complete oxidation of methane on  $\text{Co}_3\text{O}_4\text{-SnO}_2$  catalysts. *Front. Environ. Sci. Engin. China* **3**, 265-270 (2009)
17. Persson, K., Ersson, A., Jansson, K., Fierro, J. L. G. & Jaras, S. G. Influence of molar ratio on Pd-Pt catalysts for methane combustion. *J. Catal.* **243**, 14-24 (2006)
18. Yin, F. X., Ji, S. F., Wu, P. Y., Zhao, F. Z. & Li, C. Y. Deactivation behavior of Pd-based SBA-15 mesoporous silica catalysts for the catalytic combustion of methane. *J. Catal.* **257**, 108-116 (2008)
19. Rui, Z. B., Huang, Y. F., Zheng, Y., Ji, H. B. & Yu, X. Effect of titania polymorph on the properties of CuO/TiO<sub>2</sub> catalysts for trace methane combustion. *J. Mol. Catal. A* **372**, 128-136 (2013)
20. Park, J. H. *et al.* Methane combustion over Pd catalysts loaded on medium and large pore zeolites. *Top. Catal.* **52**, 27-34 (2009)

21. Hu, L. H., Peng, Q. & Li, Y. D. Selective synthesis of  $\text{Co}_3\text{O}_4$  nanocrystal with different shape and crystal plane effect on catalytic property for methane combustion. *J. Am. Chem. Soc.* **130**, 16136-16137 (2008)
22. Fei, Z. Y., He, S. C., Li, L., Ji, W. J. & Au, C. T. Morphology-directed synthesis of  $\text{Co}_3\text{O}_4$  nanotubes based on modified Kirkendall effect and its application in  $\text{CH}_4$  combustion. *Chem. Commun.* **48**, 853-855 (2012)
23. Li, H. F. *et al.* Catalytic methane combustion over  $\text{Co}_3\text{O}_4/\text{CeO}_2$  composite oxides prepared by modified citrate Sol-Gel method. *Catal. Lett.* **141**, 452-458 (2011)
24. Liotta, L. F., Di Carlo, G., Pantaleo, G., Venezia, A. M. & Deganello, G.  $\text{Co}_3\text{O}_4/\text{CeO}_2$  composite oxides for methane emissions abatement: Relationship between  $\text{Co}_3\text{O}_4$ - $\text{CeO}_2$  interaction and catalytic activity. *Appl. Catal. B* **66**, 217-227 (2006)
25. Zavyalova, U., Scholz, P. & Ondruschka, B. Influence of cobalt precursor and fuels on the performance of combustion synthesized  $\text{Co}_3\text{O}_4/\gamma\text{-Al}_2\text{O}_3$  catalysts for total oxidation of methane. *Appl. Catal. A* **323**, 226-233 (2007)
26. Iamarino, M., Chirone, R., Pirone, R., Russo, G. & Salatino, P. Catalytic combustion of methane in a fluidized bed reactor under fuel-lean conditions. *Combust. Sci. Technol.* **174**, 361-375 (2002)
27. Jiang, Z. *et al.* Catalytic combustion of methane over mixed oxides derived from Co-Mg/Al ternary hydrotalcites. *Fuel Process. Technol.* **91**, 97-102 (2010)
28. Baiker, A., Marti, P. E., Keusch, P., Fritsch, E. & Reller, A. Influence of the a-Site Cation in  $\text{ACoO}_3$  (a=La, Pr, Nd, and Gd) Perovskite-Type Oxides on Catalytic Activity for Methane Combustion. *J. Catal.* **146**, 268-276 (1994)
29. Cimino, S. *et al.* Methane combustion and CO oxidation on zirconia-supported La, Mn oxides and  $\text{LaMnO}_3$  perovskite. *J. Catal.* **205**, 309-317 (2002)
30. Beck, I. E. *et al.* Platinum nanoparticles on  $\text{Al}_2\text{O}_3$ : Correlation between the particle size and activity in total methane oxidation. *J. Catal.* **268**, 60-67 (2009)
31. Yao, Y. F. Y. Oxidation of Alkanes over Noble-Metal Catalysts. *Ind. Eng. Chem. Prod. Res. Dev.* **19**, 293-298 (1980)
32. Zhu, G. H., Han, J. Y., Zemlyanov, D. Y. & Ribeiro, F. H. The turnover rate for the catalytic combustion of methane over palladium is not sensitive to the structure of the catalyst. *J. Am. Chem. Soc.* **126**, 9896-9897 (2004)
33. Cullis, C. F. & Willatt, B. M. Oxidation of Methane over Supported Precious Metal-Catalysts. *J. Catal.* **83**, 267-285 (1983)
34. Xu, J. *et al.* Operando and Kinetic Study of Low-Temperature, Lean-Burn Methane Combustion over a  $\text{Pd}/\gamma\text{-Al}_2\text{O}_3$  Catalyst. *ACS Catal.* **2**, 261-269 (2012)
35. Ribeiro, F. H., Chow, M. & Dallabetta, R. A. Kinetics of the Complete Oxidation of Methane over Supported Palladium Catalysts. *J. Catal.* **146**, 537-544 (1994)
36. Zhu, Z. Z. *et al.* Highly active and stable  $\text{Co}_3\text{O}_4/\text{ZSM}-5$  catalyst for propane oxidation: effect of the preparation method. *ACS Catal.* **3**, 1154-1164 (2013)